ARTHRITIS & RHEUMATOLOGY
Vol. 67, No. 3, March 2015, pp 656–667
DOI 10.1002/art.38975

Loss of SH3 Domain–Binding Protein 2 Function Suppresses Bone Destruction in Tumor Necrosis Factor–Driven and Collagen-Induced Arthritis in Mice

Tomoyuki Mukai,[1] Richard Gallant,[1] Shu Ishida,[2] Mizuho Kittaka,[1] Teruhito Yoshitaka,[1] David A. Fox,[3] Yoshitaka Morita,[4] Keiichiro Nishida,[5] Robert Rottapel,[6] and Yasuyoshi Ueki[1]

Objective. **SH3 domain–binding protein 2 (SH3BP2) is a signaling adapter protein that regulates the immune and skeletal systems. The present study was undertaken to investigate the role of SH3BP2 in arthritis using 2 experimental mouse models, i.e., human tumor necrosis factor α–transgenic (hTNF-Tg) mice and mice with collagen-induced arthritis (CIA).**

Methods. **First, Sh3bp2$^{-/-}$ and wild-type (Sh3bp2$^{+/+}$) mice were crossed with hTNF-Tg mice. Inflammation and bone loss were examined by clinical inspection and histologic and micro–computed tomography analysis, and osteoclastogenesis was evaluated using primary bone marrow–derived macrophage colony-stimulating factor–dependent macrophages (BMMs). Second, CIA was induced in Sh3bp2$^{-/-}$ and Sh3bp2$^{+/+}$ mice, and the incidence and severity of arthritis were evaluated. Anti–mouse type II collagen (CII) antibody levels were measured by enzyme-linked immunosorbent assay, and lymph node cell responses to CII were determined.**

Results. **SH3BP2 deficiency did not alter the severity of joint swelling but did suppress bone erosion in the hTNF-Tg mouse model. Bone loss at the talus and tibia was prevented in Sh3bp2$^{-/-}$/hTNF-Tg mice compared to Sh3bp2$^{+/+}$/hTNF-Tg mice. RANKL- and TNFα-induced osteoclastogenesis was suppressed in Sh3bp2$^{-/-}$ mouse BMM cultures. NF-ATc1 nuclear localization in response to TNFα was decreased in Sh3bp2$^{-/-}$ mouse BMMs compared to Sh3bp2$^{+/+}$ mouse BMMs. In the CIA model, SH3BP2 deficiency suppressed the incidence of arthritis and this was associated with decreased anti-CII antibody production, while antigen-specific T cell responses in lymph nodes were not significantly different between Sh3bp2$^{+/+}$ and Sh3bp2$^{-/-}$ mice.**

Conclusion. **SH3BP2 deficiency prevents loss of bone via impaired osteoclastogenesis in the hTNF-Tg mouse model and suppresses the induction of arthritis via decreased autoantibody production in the CIA model. Therefore, SH3BP2 could potentially be a therapeutic target in rheumatoid arthritis.**

Rheumatoid arthritis (RA) is a chronic inflammatory bone-destructive disorder with autoimmune features. It is driven by diverse cellular and humoral immune responses, resulting in bone destruction. Bone loss in RA is caused by osteoclasts (1–3). Osteoclast differentiation is controlled mainly by RANK and its ligand, RANKL. RANKL is expressed on osteoblasts and can be expressed by other cells, such as fibroblasts and T cells, in inflammatory conditions (4–6). In RA, tumor necrosis factor α (TNFα) augments RANKL expression in synovial fibroblasts and subsequently enhances osteoclastogenesis in inflamed joints (4–6). Ad-

Supported by the Japan Rheumatism Foundation (Rheumatology Traveling Fellowship to Dr. Mukai), Kawasaki Medical School (Research Project Grant 26-75 to Dr. Morita), the Canadian Institute for Health Research (grant to Dr. Rottapel), and the NIH (grant R01-DE-020835 to Dr. Ueki).

[1]Tomoyuki Mukai, MD, PhD, Richard Gallant, BA, Mizuho Kittaka, DDS, PhD, Teruhito Yoshitaka, MD, PhD, Yasuyoshi Ueki, MD, PhD: University of Missouri–Kansas City; [2]Shu Ishida, DDS: University of Missouri–Kansas City and Hiroshima University Graduate School of Biomedical Sciences, Hiroshima, Japan; [3]David A. Fox, MD: University of Michigan, Ann Arbor; [4]Yoshitaka Morita, MD, PhD: Kawasaki Medical School, Kurashiki, Japan; [5]Keiichiro Nishida, MD, PhD: Okayama University Graduate School of Medicine, Dentistry and Pharmaceutical Sciences, Okayama, Japan; [6]Robert Rottapel, MD, FRCPC: University of Toronto and Saint Michael's Hospital, Toronto, Ontario, Canada.

Address correspondence to Yasuyoshi Ueki, MD, PhD, Department of Oral and Craniofacial Sciences, School of Dentistry, University of Missouri–Kansas City, 650 East 25th Street, Kansas City, MO 64108. E-mail: uekiy@umkc.edu.

Submitted for publication May 7, 2014; accepted in revised form November 25, 2014.

ditionally, TNFα enhances osteoclastogenesis by acting on osteoclast precursors directly or synergistically with RANKL (7–10). Excessive osteoclast activity consequently causes local and systemic bone loss (11,12). Additionally, one of the characteristic features of RA is the presence of autoantibodies, notably rheumatoid factor and anti–citrullinated protein antibodies (3,13). Autoantibody production by B cells is a major pathogenic mechanism leading to chronic inflammation in RA.

SH3 domain–binding protein 2 (SH3BP2) is an adapter protein that is expressed primarily in immune cells including T cells, B cells, and macrophages, as well as osteoclasts. It interacts with various proteins, including Syk (14), phospholipase Cγ (14,15), and Src (16,17), and regulates intracellular signaling pathways in the immune and skeletal systems (18–21). It has previously been reported (22,23) that gain-of-function mutations in Sh3bp2 cause cherubism (OMIM no. #118400), a human craniofacial disorder characterized by excessive jawbone destruction (24). The jaw lesions in cherubism consist mainly of fibroblastoid cells with numerous tartrate-resistant acid phosphatase (TRAP)–positive multinucleated giant cells (24,25), suggesting that the excessive bone resorption is caused by increased osteoclast formation.

A mouse model of cherubism has been generated by knocking-in a P416R Sh3bp2 mutation (equivalent to the most common P418R mutation in cherubism patients) (21). Analysis of the mouse model has revealed that heterozygous ($Sh3bp2^{P416R/+}$) mice exhibit osteopenia due to increased RANKL-induced osteoclastogenesis (21). Unexpectedly, homozygous mutants ($Sh3bp2^{P416R/P416R}$ mice) spontaneously develop severe arthritis. In SH3BP2-deficient mice, B cell proliferation and signaling in response to B cell antigen receptor ligation have been shown to be impaired, although no abnormalities in T cell function were observed (18,19). Furthermore, SH3BP2 loss-of-function suppresses RANKL-induced osteoclastogenesis (16,17,26). These findings suggest a potential pathologic link between SH3BP2 and arthritis, through the SH3BP2-induced modulation of osteoclastogenesis and autoimmune reactions. However, the exact mechanisms by which SH3BP2 regulates arthritis have not been clarified.

In this study, we hypothesized that SH3BP2 plays a role in the pathogenesis of bone-destructive inflammatory diseases such as RA, in which TNFα and autoantibody production are critically involved (3). To test this hypothesis, we used 2 different murine arthritis models, a human TNFα–transgenic (hTNF-Tg) mouse model (27,28) and a collagen-induced arthritis (CIA) model (29,30). We demonstrated that SH3BP2 deficiency prevents bone loss via impaired osteoclastogenesis in the hTNF-Tg model and suppresses the induction of arthritis via decreased autoantibody production in the CIA model.

MATERIALS AND METHODS

Mice. TNF-Tg mice (C57BL/6 background) were obtained from Taconic (27) and crossed with $Sh3bp2^{-/-}$ mice (C57BL/6 background) (18). DBA/1J mice were purchased from The Jackson Laboratory. $Sh3bp2^{-/-}$ mice were backcrossed for 10 generations onto a DBA/1 background and used for CIA experiments. Mice were housed in a specific pathogen–free facility. All experimental procedures were approved by the Institutional Animal Care and Use Committees.

Reagents. Recombinant murine macrophage colony-stimulating factor (M-CSF), RANKL, and TNFα were obtained from PeproTech. Chick type II collagen (CII), Freund's complete adjuvant (CFA), and anti–mouse CII antibody assay kits were purchased from Chondrex.

Evaluation of arthritis in hTNF-Tg mice. Arthritis severity in $Sh3bp2^{+/+}$/hTNF-Tg and $Sh3bp2^{-/-}$/hTNF-Tg mice was scored, under blinded conditions, once per week until 16 weeks of age, using the following criteria: 0 = normal; 1 = mild erythema or swelling of the wrist or ankle, or erythema and swelling of 1 digit; 2 = moderate erythema and swelling of the wrist or ankle, or >3 inflamed digits; 3 = severe erythema and swelling of the wrist or ankle; and 4 = complete erythema and swelling of the wrist and ankle, including all digits. Each limb was graded separately, yielding a maximum possible total score of 16. At 16 weeks of age, the mice were killed and serum and hind limbs were collected. Serum concentrations of human and mouse TNFα were measured by enzyme-linked immunosorbent assay (ELISA; R&D Systems). After fixation with 4% paraformaldehyde in phosphate buffered saline, hind limbs were assessed radiologically and histologically.

Histologic and histomorphometric analysis. Hind limbs were decalcified in 0.5*M* EDTA (pH 7.2) at 4°C for 4 weeks and embedded in paraffin. Sections (6 μm) were stained with hematoxylin and eosin and Safranin O. The severity of inflammation and of cartilage damage was scored, under blinded conditions, by 2 independent observers (TM and RG) using the following criteria: for inflammation, 0 = normal; 1 = mild diffuse inflammatory infiltrates; 2 = moderate inflammatory infiltrates; 3 = marked inflammatory infiltrates; and 4 = severe inflammation with pannus formation; for cartilage damage, 0 = normal; 1 = mild loss of Safranin O staining with no obvious chondrocyte loss; 2 = moderate loss of staining with focal mild chondrocyte loss; 3 = marked loss of staining with multifocal marked chondrocyte loss; and 4 = severe diffuse loss of staining with multifocal severe chondrocyte loss. TRAP staining with methyl green counterstaining was performed to visualize TRAP+ cells. Histomorphometric measurements were performed using OsteoMeasure software (OsteoMetrics). TRAP+ multinucleated cells (MNCs) containing ≥3 nuclei were defined as osteoclasts. Eroded surface/bone surface (ES/BS) and osteoclast number/bone surface

(N.Oc/BS) of talus were determined. The terminology used and units reported were based on international guidelines (31).

Micro–computed tomographic (micro-CT) analysis. Left hind limbs were scanned with a vivaCT 40 (Scanco Medical). The threshold was set to 300 for hind paw bone, 260 for cortical bone of the tibia, and 220 for trabecular bone of the tibia to distinguish mineralized tissue. Talar bone volume was quantified to evaluate bone erosion (32). The regions of tibial trabecular and cortical bone were selected as described previously (33). All micro-CT parameters were consistent with international guidelines (34).

Osteoclast differentiation assay. Primary bone marrow cell culture was performed as previously described (21). Mouse bone marrow cells were isolated from long bones of 9-week-old female Sh3bp2$^{+/+}$ and Sh3bp2$^{-/-}$ mice and cultured on petri dishes for 2–4 hours. Nonadherent cells were reseeded on 48-well plates at 2.1×10^4 cells/well and incubated at 37°C/5% CO_2 for 2 days in α-minimum essential medium/10% fetal bovine serum containing M-CSF (25 ng/ml). Bone marrow–derived M-CSF–dependent macrophages (BMMs) were stimulated with RANKL and TNFα in the presence of M-CSF (25 ng/ml) for an additional 4 days. Culture media were changed every other day. TRAP+ MNCs ($\geq$3 nuclei) were visualized by TRAP staining (Sigma-Aldrich) and counted at 40× magnification (n = 4–6 wells/group).

Resorption assay. Dentin slices were sterilized in 70% ethanol, washed with phosphate buffered saline, and placed on the bottom of 96-well plates. Nonadherent bone marrow cells were plated at 8.5×10^3 cells/well. After 2-day preculture with M-CSF, BMMs were stimulated with RANKL and TNFα in the presence of M-CSF (25 ng/ml) for 14 days. After removal of the cells with 1*M* NH_4OH, resorption areas were visualized with toluidine blue, followed by quantification with ImageJ (National Institutes of Health).

Real-time quantitative polymerase chain reaction (PCR). Total RNA was extracted using TRIzol (Invitrogen). Complementary DNA was transcribed with High Capacity cDNA Reverse Transcription Kits (Applied Biosystems). Quantitative PCR was performed using Absolute Blue qPCR Master Mix (Thermo Scientific) with a StepOne Plus system (Applied Biosystems). Gene expression levels relative to Hprt were calculated by the $\Delta\Delta C_t$ method and were normalized to baseline controls. Primers were as follows: Tnfa 5′-CATCTTCTCAAAATTCGAGTGACA-3′ (forward), 5′-TGGGAGTAGACAAGGTACAACCC-3′ (reverse); Acp5 5′-CAGCAGCCCAAAATGCCT-3′ (forward), 5′-TTTTGAGCCAGGACAGCTGA-3′ (reverse); Ctsk 5′-CGAAAAGAGCCTAGCGAACA-3′ (forward), 5′-TGGGTAGCAGCAGAAACTTG-3′ (reverse); Oscar 5′-TCTGCCCCCTATGTGCTATCA-3′ (forward), 5′-AGGAGCCAGAACCTTCGAAAC-3′ (reverse); Hprt, 5′-TCCTCCTCAGACCGCTTTT-3′ (forward), 5′-CCTGGTTCATCATCGCTAATC-3′ (reverse). All quantitative PCRs yielded products with single-peak dissociation curves.

Western blotting. For nuclear and cytoplasmic fractionation, BMMs were lysed on ice in cytoplasmic lysis buffer with protease inhibitors (Sigma-Aldrich), and nuclei were lysed in nuclear lysis buffer as described previously (33). Nuclear protein (1 μg/lane) and cytoplasmic protein (4 μg/lane) were resolved by sodium dodecyl sulfate–polyacrylamide gel electrophoresis and transferred to nitrocellulose membranes. After blocking with 5% skim milk, membranes were incubated with primary antibodies and then with horseradish peroxidase–conjugated secondary antibodies (Cell Signaling Technology). Bands were detected using SuperSignal West chemiluminescent substrates (Thermo Scientific) and visualized with LAS-4000 (GE Healthcare).

Induction of CIA. Nine-week-old male Sh3bp2$^{+/+}$ and Sh3bp2$^{-/-}$ mice (DBA/1 background) were injected intradermally with 100 μg chick CII with CFA at the base of the tail on day 0 (35,36). On day 21, a booster injection of 100 μg chick CII in Freund's incomplete adjuvant was administered. Arthritis severity was assessed, under blinded conditions, twice per week until day 70, using the same criteria as were applied for the hTNF-Tg mice.

ELISA for anti–mouse CII antibody. Serum levels of anti–mouse CII antibody (total IgG, IgG1, IgG2a, and IgG2b) were measured according to the protocol recommended by the manufacturer of the ELISA Kit (Chondrex). Diluted serum samples were added to mouse CII–coated 96-well plates and incubated at 4°C overnight. Bound IgG was detected by incubation with horseradish peroxidase–conjugated anti-mouse IgG followed by *o*-phenylenediamine substrate.

Cell proliferation and cytokine production in draining lymph node cell culture. Nine-week-old male Sh3bp2$^{+/+}$ and Sh3bp2$^{-/-}$mice were immunized with 100 μg chick CII in CFA. Ten days after immunization, inguinal lymph nodes were isolated. Lymph node cells were cultured at 4×10^5 cells/well in 96-well U-bottomed plates in RPMI1640 with 10% heat-inactivated fetal bovine serum, 50 μM 2-mercaptoethanol, and 1% L-glutamine at 37°C/5% CO_2 (37). The cells were stimulated for 72 hours with 50 μg/ml denatured chick CII. Cell proliferation was determined using CellTiter 96 Proliferation Assay (MTS) reagent according to the instructions of the manufacturer (Promega). Levels of interferon-γ (IFNγ) and interleukin-17 (IL-17) in media were determined by ELISA (R&D Systems).

Statistical analysis. Mean ± SEM values were determined, and statistical analysis was performed by Student's unpaired 2-tailed *t*-test to compare 2 groups and by one-way analysis of variance with Tukey-Kramer post hoc test to compare 3 or more groups. The significance of differences in arthritis incidence rates was assessed by Fisher's exact test. GraphPad Prism 5 was used for all statistical analyses. *P* values less than 0.05 were considered significant.

RESULTS

Suppressed bone erosion in Sh3bp2-deficient hTNF-Tg mice. To investigate the role of SH3BP2 in the pathogenesis of arthritis, we crossed SH3BP2-deficient mice with hTNF-Tg mice, which spontaneously produce TNFα and develop TNFα-dependent arthritis (27,28). We found that both Sh3bp2$^{+/+}$/hTNF-Tg and Sh3bp2$^{-/-}$/hTNF-Tg mice developed severe arthritis and that the severity of arthritis was comparable between them (Figure 1A). Serum levels of human and murine TNFα were also similar in Sh3bp2$^{+/+}$/hTNF-Tg and Sh3bp2$^{-/-}$/hTNF-Tg mice (Figure 1B). These data suggest that SH3BP2 defi-

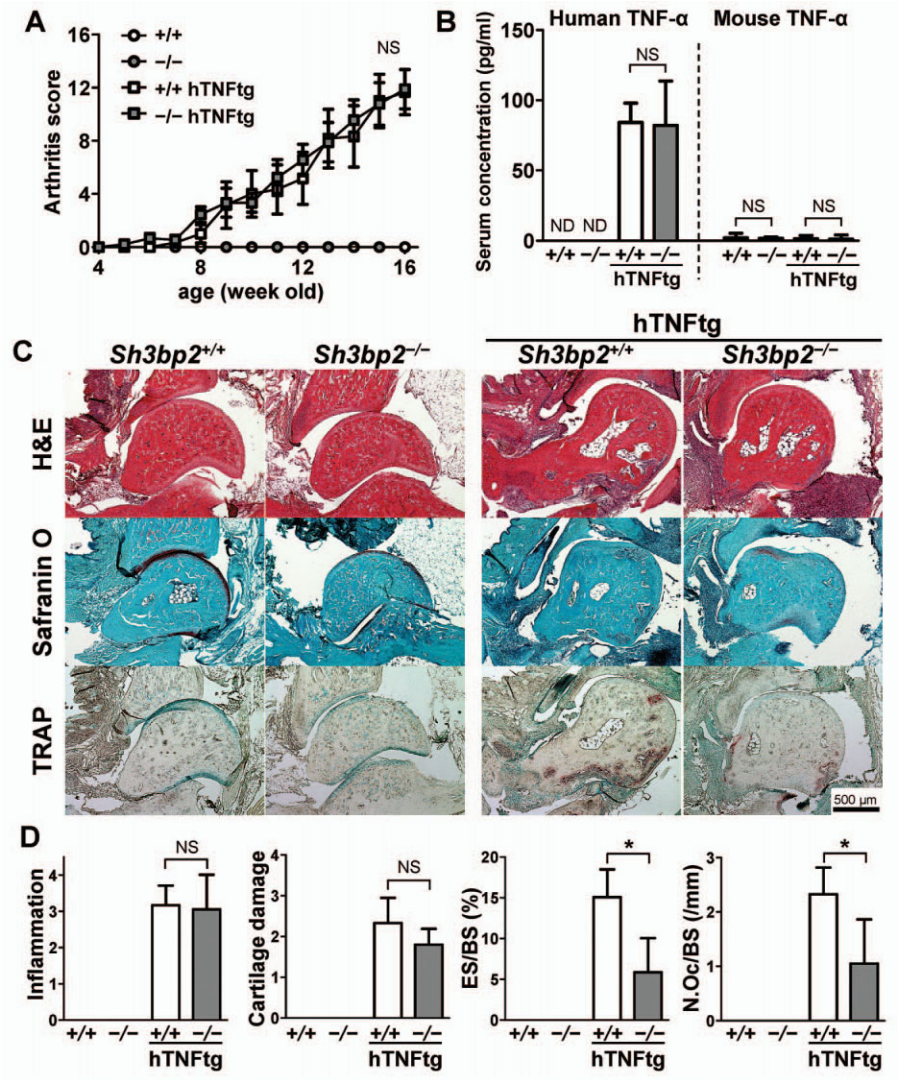

Figure 1. Decreased osteoclast formation and bone erosion in SH3BP2-deficient human tumor necrosis factor α–transgenic (hTNF-Tg) mice. $Sh3bp2^{+/+}$ (+/+) and $Sh3bp2^{-/-}$ (−/−) mice were crossed with hTNF-Tg mice. Joint inflammation was monitored through age 16 weeks, at which time the mice were killed and serum and hind limbs collected for analysis. **A,** Clinically assessed joint inflammation scores in male $Sh3bp2^{+/+}$ and $Sh3bp2^{-/-}$ mice (n = 9 and n = 7, respectively) and $Sh3bp2^{+/+}$/hTNF-Tg and $Sh3bp2^{-/-}$/hTNF-Tg mice (n = 7 and n = 9, respectively). **B,** Serum concentrations of human and mouse TNFα in the 4 groups. **C,** Representative results of staining of ankle joint tissue from mice in the 4 groups. Ankle joint sections were stained with hematoxylin and eosin (H&E), Safranin O, and tartrate-resistant acid phosphatase (TRAP). Original magnification × 40. **D,** Histologic scores of inflammation and cartilage damage and results of talar bone histomorphometric analysis (eroded surface/bone surface [ES/BS] and osteoclast number/bone surface [N.Oc/BS]) of mice in the 4 groups. Bone erosion on the surface of the talus was traced, and attached osteoclasts were counted. Values are the mean ± SEM. $* = P < 0.05$. NS = not significant; ND = not detectable.

ciency does not significantly affect the severity of joint inflammation and systemic TNFα production.

Next, we examined the severity of inflammatory cell infiltration, cartilage damage, and bone erosion in tibiotalar joints. Histologic examination showed that both $Sh3bp2^{+/+}$/hTNF-Tg mice and $Sh3bp2^{-/-}$/hTNF-Tg mice developed severe inflammation, but $Sh3bp2^{-/-}$/hTNF-Tg mice exhibited less bone erosion (Figure 1C). Quantitative histologic analysis revealed that the inflammation score and the cartilage damage score were comparable between $Sh3bp2^{+/+}$/hTNF-Tg and $Sh3bp2^{-/-}$/hTNF-Tg mice (Figure 1D). Histomorphometric analysis, in contrast, showed that ES/BS and N.Oc/BS were lower in $Sh3bp2^{-/-}$/hTNF-Tg mice than

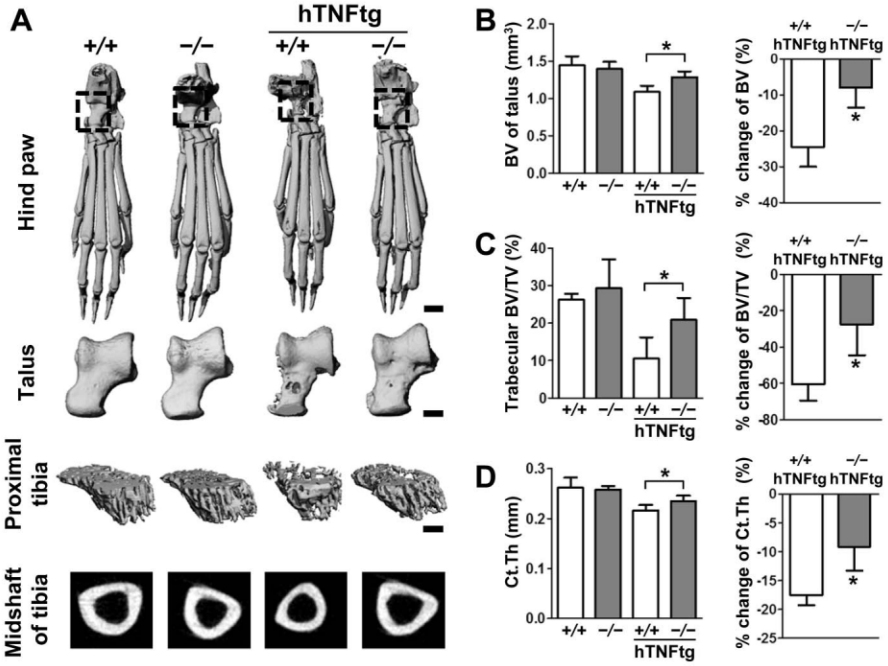

Figure 2. Reduction of focal and systemic bone loss in SH3BP2-deficient human tumor necrosis factor α–transgenic (hTNF-Tg) mice. Male Sh3bp2$^{+/+}$ (+/+) and Sh3bp2$^{-/-}$ (−/−) mice (n = 9 and n = 7, respectively), and Sh3bp2$^{+/+}$/hTNF-Tg and Sh3bp2$^{-/-}$/hTNF-Tg mice (n = 7 and n = 9, respectively) were killed at age 16 weeks, and left hind limbs were collected. The hind paws and tibiae were analyzed by micro–computed tomography (micro-CT). **A,** Representative micro-CT images of hind paws, talar bones, and trabecular and cortical bones of the tibiae. Bars = 1 mm (hind paw) and 400 μm (talus and tibia). **B,** Bone volume (BV) of the talus and percent change in BV relative to control Sh3bp2$^{+/+}$ and Sh3bp2$^{-/-}$ mice. **C,** Bone volume/total volume (BV/TV) in trabecular bone of proximal tibia and percent change in trabecular BV/TV relative to control Sh3bp2$^{+/+}$ and Sh3bp2$^{-/-}$ mice. **D,** Cortical thickness (Ct.Th) of the midshaft of the tibia and percent change in Ct.Th relative to control Sh3bp2$^{+/+}$ and Sh3bp2$^{-/-}$ mice. Values are the mean ± SEM. $* = P < 0.05$ versus Sh3bp2$^{+/+}$/hTNF-Tg mice.

in Sh3bp2$^{+/+}$/hTNF-Tg mice (Figure 1D). These findings indicate that SH3BP2 deficiency suppresses osteoclast formation and bone erosion in inflamed joints without significantly affecting the severity of inflammation.

Decreased focal and systemic bone loss in SH3BP2-deficient hTNF-Tg mice. Arthritic conditions cause focal bone loss in inflamed joints, as well as systemic bone loss (11,12). We assessed the bone properties of the talus and the tibia as parameters of focal and systemic bone loss, respectively. Micro-CT analysis revealed bone erosion on the talus of both Sh3bp2$^{+/+}$/hTNF-Tg and Sh3bp2$^{-/-}$/hTNF-Tg mice, but the erosion was milder in the Sh3bp2$^{-/-}$/hTNF-Tg mice (Figure 2A). To quantify the focal bone loss, the bone volume (BV) of the talus and the percent change in BV of the talus relative to that in noninflamed tali from control mice were determined as previously described (32). The average BV of the talus was greater in Sh3bp2$^{-/-}$/hTNF-Tg mice than in Sh3bp2$^{+/+}$/hTNF-Tg mice, and the percent change in BV of the talus was less in Sh3bp2$^{-/-}$/hTNF-Tg mice (Figure 2B). To examine whether SH3BP2 deficiency suppresses systemic bone loss, properties of trabecular and cortical bone of the tibia were determined. We found that bone volume/total volume was greater in Sh3bp2$^{-/-}$/hTNF-Tg mice than in Sh3bp2$^{+/+}$/hTNF-Tg mice, and the rate of trabecular bone loss was smaller in Sh3bp2$^{-/-}$/hTNF-Tg mice than in Sh3bp2$^{+/+}$/hTNF-Tg mice (Figure 2C). The results were similar when cortical thickness of the tibia was measured (Figure 2D). Taken together, these data show that loss-of-function of SH3BP2 prevents focal and systemic bone loss in the hTNF-Tg arthritis model.

TNFα messenger RNA (mRNA) expression in primary BMMs. It has previously been reported that SH3BP2 plays a role in TNFα production by macrophages, as demonstrated by the observation that the P416R Sh3bp2 gain-of-function mutation in macrophages resulted in greater TNFα production in response to M-CSF compared to that observed in Sh3bp2$^{+/+}$ mouse macrophages (21). To examine whether SH3BP2 deficiency suppresses TNFα expression in macrophages,

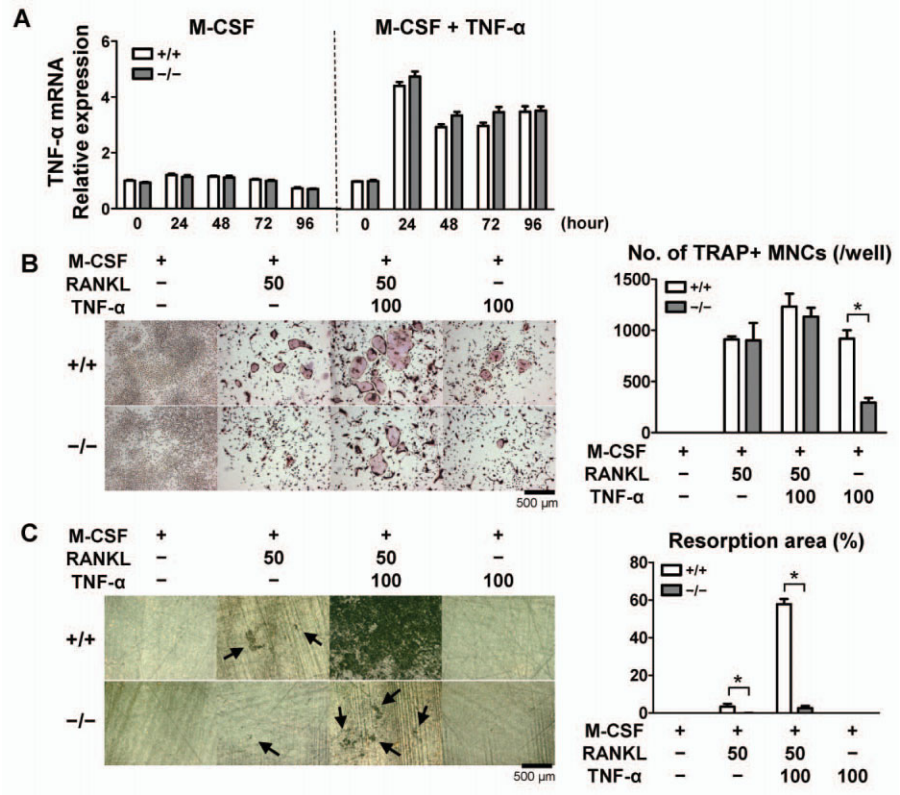

Figure 3. Impaired osteoclast differentiation and bone-resorbing function in Sh3bp2$^{-/-}$ (−/−) bone marrow–derived macrophages (BMMs). Primary bone marrow cells were isolated and cultured as described in Materials and Methods. **A,** Expression of mRNA for tumor necrosis factor α (TNFα). BMMs were stimulated with TNFα (100 ng/ml) in the presence of macrophage colony-stimulating factor (M-CSF; 25 ng/ml). TNFα mRNA expression levels relative to Hprt were calculated and normalized to the expression level in Sh3bp2$^{+/+}$ (+/+) BMMs at time 0. **B,** Representative images showing tartrate-resistant acid phosphatase (TRAP) staining under the different experimental conditions, and number of TRAP+ multinucleated cells (MNCs). BMMs were stimulated for 4 days with RANKL alone (50 ng/ml), the combination of RANKL (50 ng/ml) and TNFα (100 ng/ml), or TNFα alone (100 ng/ml) in the presence of M-CSF (25 ng/ml). Original magnification × 40. **C,** Representative images showing bone resorption areas on dentin (**arrows** indicate resorption pits), and quantification of the percentage of resorption area relative to total surface area. BMMs were stimulated for 14 days with RANKL (50 ng/ml) and/or TNFα (100 ng/ml) in the presence of M-CSF (25 ng/ml). After removal of the cells, resorption areas were visualized with toluidine blue. Values are the mean ± SEM. $* = P < 0.05$. Original magnification × 40 in **B**; × 50 in **C**. Color figure can be viewed in the online issue, which is available at http://onlinelibrary.wiley.com/doi/10.1002/art.38975/abstract.

we measured TNFα mRNA expression levels in Sh3bp2$^{+/+}$ and Sh3bp2$^{-/-}$ mouse BMMs in response to M-CSF and TNFα. Stimulation with M-CSF alone did not increase the expression of mRNA for TNFα during the culture period (Figure 3A). TNFα and M-CSF together increased TNFα mRNA expression (4-fold increase at 24 hours after treatment), but expression levels were comparable between Sh3bp2$^{+/+}$ and Sh3bp2$^{-/-}$ mouse BMMs (Figure 3A). These results suggest that SH3BP2 deficiency does not significantly alter TNFα expression in BMMs, consistent with the absence of a difference in serum TNFα levels between Sh3bp2$^{+/+}$/hTNF-Tg and Sh3bp2$^{-/-}$/hTNF-Tg mice (Figure 1B).

Impaired osteoclastogenesis in SH3BP2-deficient primary BMMs. Decreased osteoclast formation and bone erosion in the inflamed joints of Sh3bp2$^{-/-}$ mice led us to investigate the role of SH3BP2 in osteoclastogenesis. Since RANKL and TNFα are involved in the mechanisms of inflammatory bone resorption (4–6), we focused on RANKL- and TNFα-induced osteoclastogenesis. Sh3bp2$^{+/+}$ and Sh3bp2$^{-/-}$ mouse BMMs were stimulated with RANKL and/or TNFα in the presence of M-CSF. We found that cell proliferation was compa-

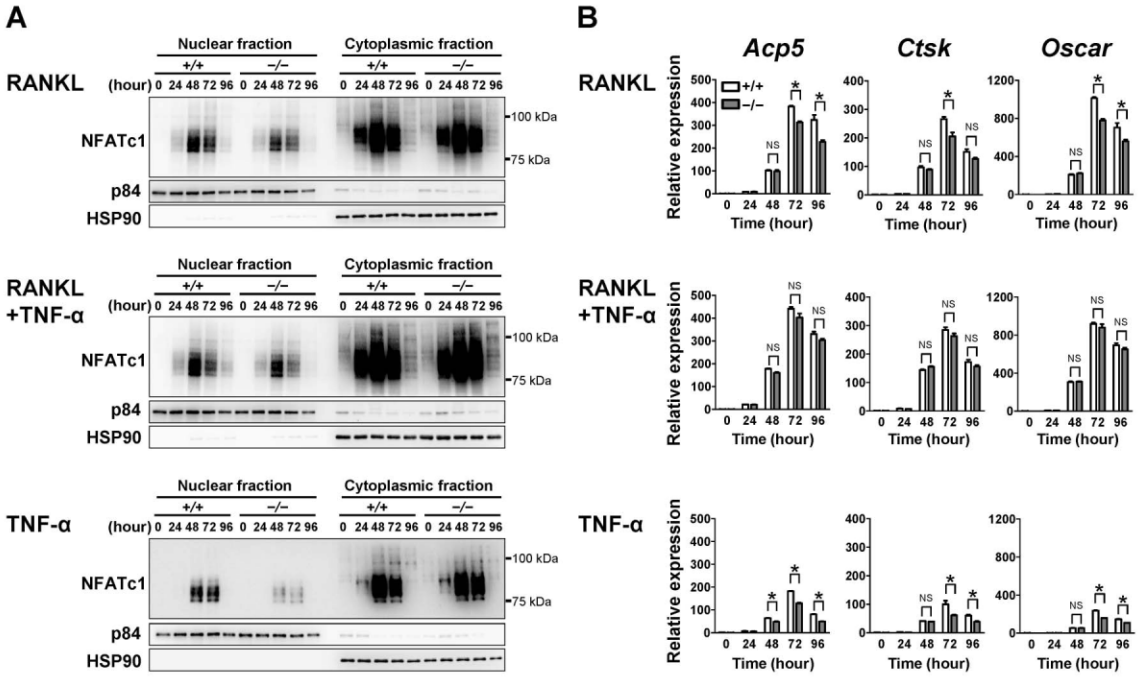

Figure 4. Reduced NF-ATc1 nuclear localization in Sh3bp2$^{-/-}$ mouse BMMs treated with TNFα. BMMs were stimulated with RANKL alone (50 ng/ml), the combination of RANKL (50 ng/ml) and TNFα (100 ng/ml), or TNFα alone (100 ng/ml) in the presence of M-CSF (25 ng/ml). **A,** Western blot analysis of NF-ATc1. Nuclear and cytoplasmic protein samples were isolated at the indicated time points after stimulation. Nuclear matrix protein p84 and Hsp90 were used as loading controls. **B,** Quantitative polymerase chain reaction analysis of the expression of Acp5, Ctsk, and Oscar. Expression levels of mRNA for the genes relative to Hprt mRNA were calculated and normalized to the average expression levels in Sh3bp2$^{+/+}$ mouse BMMs at time 0. Values are the mean ± SEM. $* = P < 0.05$. NS = not significant (see Figure 3 for other definitions).

rable between Sh3bp2$^{+/+}$ and Sh3bp2$^{-/-}$ mouse BMMs after the stimulation (data not shown). RANKL and TNFα, alone or in combination, induced TRAP+ MNC formation in both Sh3bp2$^{+/+}$ and Sh3bp2$^{-/-}$ BMMs (Figure 3B). Sh3bp2$^{-/-}$ BMMs formed fewer TRAP+ MNCs in response to TNFα, while the numbers of TRAP+ MNCs were comparable when the BMMs were treated with RANKL or the combination of RANKL and TNFα (Figure 3B). Consistent with findings described in a previous report (16), the size of the TRAP+ MNCs from Sh3bp2$^{-/-}$ mouse BMMs was smaller than that from Sh3bp2$^{+/+}$ mouse BMMs (results not shown).

Next, we investigated the bone-resorbing function of BMMs after stimulation with RANKL and TNFα. Although TNFα alone did not induce detectable resorption pits in Sh3bp2$^{+/+}$ mouse BMM cultures, synergistically with RANKL it enhanced resorption in Sh3bp2$^{+/+}$ mouse osteoclasts (Figure 3C). In contrast, the synergistic induction of resorption pits was much lower in Sh3bp2$^{-/-}$ mouse BMMs.

Taken together, the data demonstrate that SH3BP2 deficiency reduces TRAP+ MNC formation by TNFα and inhibits osteoclastic resorbing function in response to RANKL, particularly in the presence of TNFα. These findings suggest that loss of SH3BP2 function ameliorates focal and systemic bone loss in the hTNF-Tg arthritis model by reducing the formation of functional osteoclasts in response to RANKL and TNFα.

Decreased NF-ATc1 nuclear localization in TNFα-stimulated Sh3bp2$^{-/-}$ mouse BMMs. We next investigated the mechanism by which lack of SH3BP2 impairs RANKL- and TNFα-induced osteoclastogenesis. Since previous studies have shown that SH3BP2 regulates RANKL-induced osteoclastogenesis via activation of NF-ATc1 (17,21,26,38), which is an essential transcription factor for osteoclastogenesis (38,39), we focused on levels of NF-ATc1 in BMMs. We found that nuclear expression of NF-ATc1 was decreased in Sh3bp2$^{-/-}$ mouse BMMs compared to Sh3bp2$^{+/+}$ mouse BMMs at 48–72 hours after stimulation with RANKL, TNFα, or the combination of both; this decrease was particularly marked upon stimulation with TNFα alone (Figure 4A). Nuclear expression patterns of

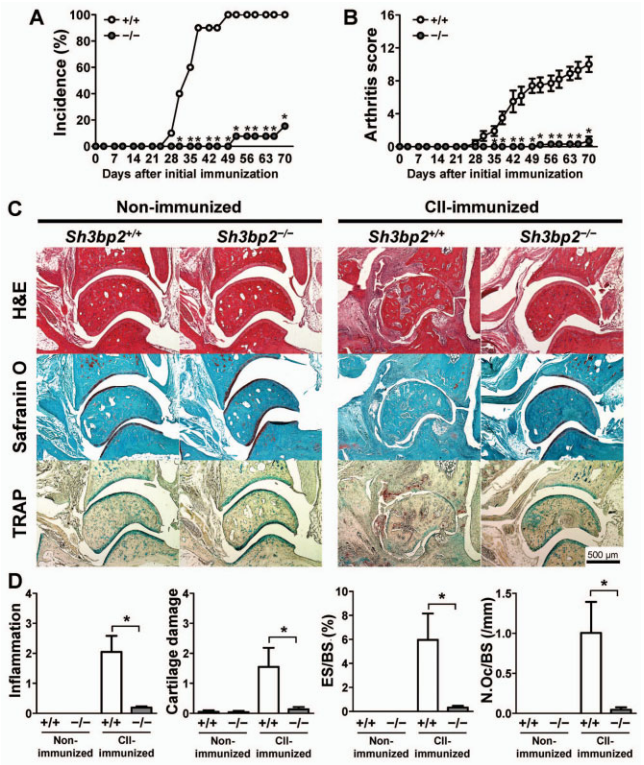

Figure 5. Decreased incidence and severity of arthritis in Sh3bp2$^{-/-}$ mice in the collagen-induced arthritis model. Nine-week-old male Sh3bp2$^{+/+}$ and Sh3bp2$^{-/-}$ mice (n = 10 and n = 13, respectively) were immunized with chick type II collagen (CII) in Freund's complete adjuvant on day 0, followed by a booster injection on day 21. Swelling of the paws was evaluated through day 70, at which time the mice were killed and hind limbs collected for analysis, with age-matched nonimmunized Sh3bp2$^{+/+}$ and Sh3bp2$^{-/-}$ mice (n = 7 and n = 7, respectively) used as controls. **A,** Incidence of arthritis. **B,** Mean ± SEM arthritis scores. **C,** Representative results of staining of ankle joint tissue from mice in the 4 groups. Ankle joint sections were stained with H&E, Safranin O, and TRAP. Original magnification × 40. **D,** Mean ± SEM histologic scores of inflammation and cartilage damage and results of talar bone histomorphometric analysis (eroded surface/bone surface and osteoclast number/bone surface) of mice in the 4 groups. Bone erosion on the surface of the talus was traced, and attached osteoclasts were counted. * = $P < 0.05$ versus Sh3bp2$^{+/+}$ mice. See Figure 1 for other definitions. Color figure can be viewed in the online issue, which is available at http://onlinelibrary.wiley.com/doi/10.1002/art.38975/abstract.

other transcription factors, such as NF-κB, c-Fos, c-Jun, and IFN regulatory factor 8, which also regulate osteoclastogenesis (40,41), in response to TNFα did not differ between Sh3bp2$^{+/+}$ and Sh3bp2$^{-/-}$ mouse BMMs (results not shown). These findings suggest that decreased NF-ATc1 nuclear localization in Sh3bp2$^{-/-}$ mouse BMMs is, at least in part, responsible for the diminished formation of active osteoclasts in vivo and in vitro.

Since osteoclast-associated genes are primarily regulated by NF-ATc1 (38), we next examined the expression of Acp5, Ctsk, and Oscar in Sh3bp2$^{+/+}$ and Sh3bp2$^{-/-}$ mouse BMMs stimulated with RANKL, TNFα, or the combination of both. We found that expression levels of the genes in Sh3bp2$^{-/-}$ mouse BMMs stimulated with RANKL or TNFα were reduced compared to expression levels in Sh3bp2$^{+/+}$ BMMs (Figure 4B). These results were similar to the previously reported finding that reduced function of SH3BP2 suppresses the expression of osteoclast-associated genes in RANKL-induced osteoclastogenesis (17,26) and support the observation that NF-ATc1 nuclear localization was decreased in TRAP+ MNCs from Sh3bp2$^{-/-}$ mice. However, expression levels of the osteoclast-associated genes were not significantly reduced in response to simultaneous stimulation with RANKL and TNFα (Figure 4B), the condition under which TRAP+ MNCs from Sh3bp2$^{-/-}$ mice exhibited a significantly decreased resorption area (Figure 3C). This suggests that SH3BP2 could regulate bone resorption independently of NF-ATc1 activation, at least in response to combined treatment with RANKL and TNFα.

Reduced incidence and severity of arthritis in CII-immunized Sh3bp2$^{-/-}$ mice. SH3BP2 is expressed in various immune cells including T and B cells (18,19), and we investigated whether SH3BP2 regulates the development of arthritis in CIA, a model in which T and B cells have essential pathogenetic roles. After immunization of Sh3bp2$^{+/+}$ and Sh3bp2$^{-/-}$ DBA/1 mice with CII, Sh3bp2$^{+/+}$ mice developed arthritis at a rate of 100% (10 of 10 mice), while the induction of arthritis in Sh3bp2$^{-/-}$ mice was significantly suppressed (15% [2 of 13 mice]) (Figure 5A). Additionally, the severity of arthritis in Sh3bp2$^{-/-}$ mice was much lower than that in Sh3bp2$^{+/+}$ mice (Figure 5B). These findings indicate that SH3BP2 deficiency suppresses the development of arthritis in the CIA model.

Decreased inflammation and cartilage damage in the joints of Sh3bp2$^{-/-}$ mice. To determine the effects of SH3BP2 deficiency on inflammation, cartilage damage, and bone erosion in the CIA model, ankle joints of CII-immunized Sh3bp2$^{+/+}$ and Sh3bp2$^{-/-}$ mice (n = 10 and n = 13, respectively) as well as nonimmunized Sh3bp2$^{+/+}$ and Sh3bp2$^{-/-}$ controls (n = 7 and n = 7, respectively) were assessed histologically. We found that CII-immunized Sh3bp2$^{+/+}$ mice developed severe inflammation, cartilage damage, and bone erosion with osteoclast formation, while inflammation, cartilage damage, and bone erosion in CII-immunized Sh3bp2$^{-/-}$ mice were much milder, with decreased osteoclast for-

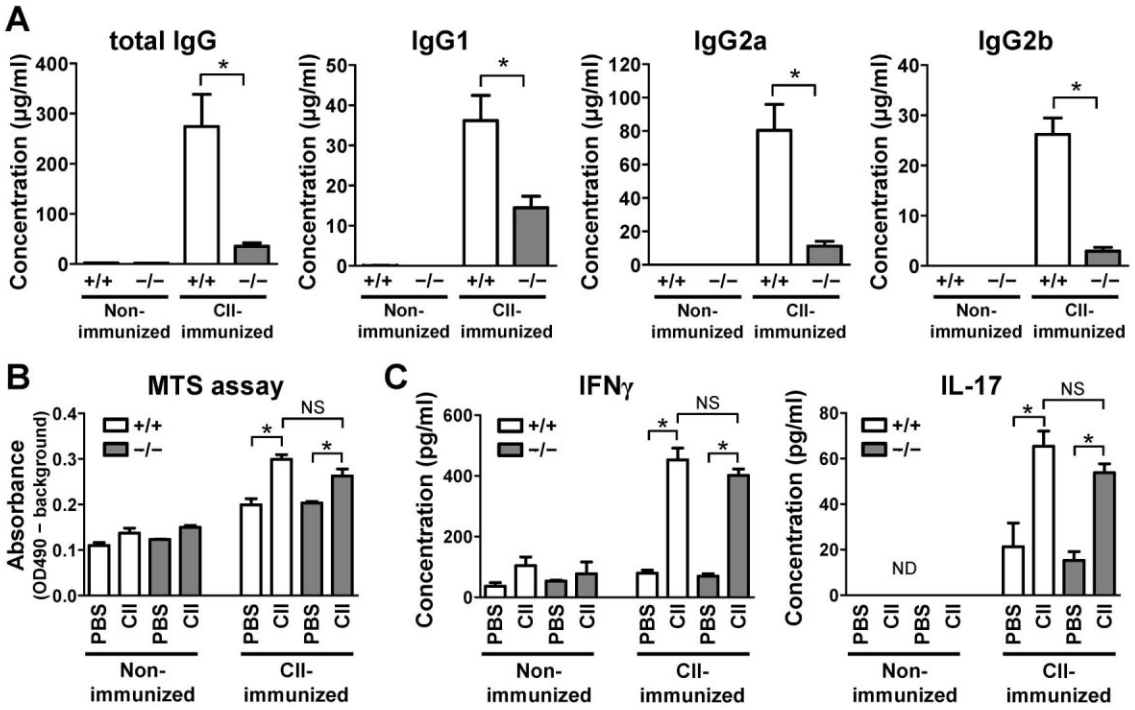

Figure 6. Impaired anti–mouse type II collagen (CII) antibody production in Sh3bp2$^{-/-}$ mice. **A,** Serum samples from male CII-immunized Sh3bp2$^{+/+}$ and Sh3bp2$^{-/-}$ mice (n = 10 and n = 13, respectively) were collected on day 70, with age-matched nonimmunized Sh3bp2$^{+/+}$ and Sh3bp2$^{-/-}$ mice (n = 7 and n = 7, respectively) used as controls. Total IgG, IgG1, IgG2a, and IgG2b anti–mouse CII were measured by enzyme-linked immunosorbent assay (ELISA). **B** and **C,** Inguinal lymph nodes from CII-immunized mice were isolated 10 days after immunization, with age-matched nonimmunized mice used as controls. Lymph node cells (4×10^5 cells/well) were stimulated with chick CII (50 μg/ml) for 72 hours. Proliferation of the cells was determined by colorimetric assay using MTS reagent (**B**), and levels of interferon-γ (IFNγ) and interleukin-17 (IL-17) in culture supernatant were measured by ELISA (lower limit of detection 10 pg/ml) (**C**). Values are the mean ± SEM. $* = P < 0.05$. PBS = phosphate buffered saline (see Figure 1 for other definitions).

mation compared to that observed in CII-immunized Sh3bp2$^{+/+}$ mice (Figure 5C). The findings were confirmed by quantitative analysis of inflammation and cartilage damage and by histomorphometric analysis (Figure 5D). These data suggest that SH3BP2 deficiency reduces the severity of inflammation, cartilage damage, and bone erosion, reflecting decreased joint inflammation and osteoclast formation, in Sh3bp2$^{-/-}$ mice.

Suppression of serum anti–mouse CII antibody levels in Sh3bp2$^{-/-}$ mice. To investigate the mechanisms underlying the suppressed induction of arthritis in Sh3bp2$^{-/-}$ mice in the CIA model, we measured levels of serum autoantibodies, which are important in the induction of CIA (29,30). As shown in Figure 6A, mouse CII total IgG levels on day 70 were increased in CII-immunized Sh3bp2$^{+/+}$ mice, while SH3BP2 deficiency dramatically suppressed the serum levels of the antibody. The IgG1, IgG2a, and IgG2b subclasses of anti-CII antibody were all decreased in CII-immunized Sh3bp2$^{-/-}$ mice as well. These results indicate that suppressed induction of arthritis in Sh3bp2$^{-/-}$ mice is associated with reduced production of anti–mouse CII antibodies.

No significant abnormality in proliferation or IFNγ and IL-17 production in Sh3bp2$^{-/-}$ draining lymph node cell cultures. T cells also play critical roles in the initiation of arthritis in the CIA model (29,30). To evaluate whether impaired T cell function is involved in the decreased development of CIA in Sh3bp2$^{-/-}$ mice, inguinal lymph nodes were isolated 10 days after immunization with CII, and cell proliferation and levels of IFNγ and IL-17 production in response to chick CII were determined. We found that cell proliferation and cytokine levels in the media were comparable between the CII-immunized Sh3bp2$^{+/+}$ and Sh3bp2$^{-/-}$ mice (Figures 6B and C). These results suggest that SH3BP2

deficiency does not significantly alter the pathogenic T cell responses in CIA, in contrast to impaired production of the associated autoantibodies.

DISCUSSION

Previous studies of SH3BP2-deficient mice have shown that, under physiologic conditions, SH3BP2 has an important role in RANKL-induced osteoclastic bone resorption (16). In the present study we demonstrated, using 2 different arthritis models, that the lack of SH3BP2 suppresses inflammatory bone destruction in hTNF-Tg mice and mice with CIA.

There is accumulating evidence suggesting that RANKL and TNFα play important roles in inflammatory bone-destructive diseases such as RA (4–6). We hypothesized that SH3BP2 contributes to RANKL- and TNFα-induced osteoclastogenesis in pathologic inflammatory conditions and obtained several pieces of evidence to support this hypothesis. First, loss-of-function of SH3BP2 ameliorated inflammatory bone destruction in hTNF-Tg mice, in conjunction with reduced numbers of TRAP+ MNCs. Second, RANKL- and TNFα-induced osteoclastogenesis was impaired in SH3BP2-deficient mouse BMMs. Third, NF-ATc1 induction and expression of osteoclast-associated genes (Acp5, Ctsk, and Oscar) in Sh3bp2$^{-/-}$ mouse BMMs were reduced in response to TNFα. In addition to its direct effect on TRAP+ MNC formation, TNFα potentiates functional osteoclast formation synergistically with RANKL (7,9,10). Based on these results, we conclude that SH3BP2 plays an important role in both RANKL- and TNFα-induced osteoclastogenesis and regulates bone destruction in pathologic inflammatory conditions by modulating responsiveness to RANKL and TNFα.

Consistent with the previous report (16), we showed that SH3BP2 deficiency suppresses RANKL-induced osteoclastic bone resorption, but not RANKL-induced TRAP+ MNC formation (Figures 3B and C). Interestingly, our study also revealed that SH3BP2 deficiency suppresses the formation of TRAP+ MNCs in response to TNFα (Figure 3B), suggesting that SH3BP2 regulates osteoclastogenesis by different mechanisms under different conditions, i.e., RANKL stimulation and TNFα stimulation. In fact, the involvement of NF-ATc1 differs between these settings. Levaot et al reported that SH3BP2 deficiency does not alter levels of NF-ATc1 nuclear localization in RANKL-stimulated BMMs (16), while we found decreased NF-ATc1 nuclear localization in TNFα-stimulated Sh3bp2$^{-/-}$ mouse BMMs. These findings suggest that SH3BP2 modulates multiple pathways in osteoclast precursors depending on the type of stimulation, presumably by interacting with different signaling molecules. Indeed, several differences in regulatory mechanisms between RANKL- and TNFα-induced osteoclastogenesis have been reported (41,42). We showed that SH3BP2 deficiency dramatically suppresses resorption area in response to combined treatment with RANKL and TNFα (Figure 3C), but exhibits a relatively small suppressive effect on nuclear NF-ATc1 localization in response to this combined treatment (Figure 4A). These findings raise the possibility that SH3BP2 could regulate bone resorption independently of NF-ATc1–mediated pathways. Further study would be needed to test this hypothesis.

Blocking of SH3BP2 function may be of benefit in the treatment of autoimmune inflammatory diseases. In the present study, we found that SH3BP2 deficiency suppresses the induction of CIA associated with decreased autoantibody production, while T cell responses against CII are not significantly affected. These results are supported by the findings of previous studies demonstrating essential roles of SH3BP2 in B cell activation. SH3BP2 has been shown to be required for optimal B cell responses without noticeably affecting T cell function in Sh3bp2$^{-/-}$ mice (18,19). In B cells, SH3BP2 regulates cell proliferation, cell cycle progression, and intracellular signaling pathways downstream of B cell antigen receptor. Intriguingly, SH3BP2 activates NF-AT in B cells through mechanisms similar to those it exerts in osteoclasts (43,44). Considering the fact that SH3BP2 deficiency reduces pathogenic autoantibody production in the CIA model, therapeutic strategies designed to suppress its function may be effective in antibody-induced diseases such as systemic lupus erythematosus or refractory immune thrombocytopenia.

Besides monocyte-lineage cells and B cells, SH3BP2 plays functional roles in various immune cells, including natural killer cells, neutrophils, and mast cells (15,45,46). Given the fact that these cells are also involved in the pathogenesis of RA (3,47–49), SH3BP2 might contribute to the development of the disease through its effects in the immune cells. Additionally, we cannot exclude the possibility that SH3BP2 regulates osteoclastogenesis indirectly via osteoblasts and synovial fibroblasts in vivo (50). To achieve better understanding of SH3BP2 function, in vitro analysis with specific cell types isolated from SH3BP2-deficient mice and analysis of SH3BP2–conditional-knockout mice or bone marrow chimera models comparing SH3BP2-deficient and wild-type mice would be beneficial.

In conclusion, we have demonstrated that lack of

SH3BP2 decreases inflammatory bone loss via impaired osteoclastogenesis in the hTNF-Tg arthritis model and that SH3BP2 deficiency suppresses induction of arthritis via decreased autoantibody production in the CIA model. These findings suggest that SH3BP2 could be a potential therapeutic target in RA. Although a direct association between SH3BP2 and RA has not yet been identified, genetic variations that affect the expression or functional level of SH3BP2 may regulate susceptibility to and severity of RA, especially through the mechanisms that control autoantibody production by B cells and bone loss by osteoclasts. Further analysis is needed to determine whether activation of SH3BP2-mediated pathways in B cells and osteoclast precursors is involved in the autoimmune and bone-destructive features of human diseases.

ACKNOWLEDGMENTS

We would like to thank Drs. Lynda Bonewald, Mark Johnson, Jeffrey Gorski, and Sarah Dallas and all staff of the Bone Biology Research Program in the Department of Oral and Craniofacial Sciences, University of Missouri–Kansas City School of Dentistry for critical discussion and helpful suggestions. We are grateful to Yixia Xie and Mark Dallas for technical assistance. We are also indebted to the staff of the University of Missouri−Kansas City Laboratory Animal Research Core for animal care.

AUTHOR CONTRIBUTIONS

All authors were involved in drafting the article or revising it critically for important intellectual content, and all authors approved the final version to be published. Dr. Ueki had full access to all of the data in the study and takes responsibility for the integrity of the data and the accuracy of the data analysis.

Study conception and design. Mukai, Morita, Nishida, Ueki.

Acquisition of data. Mukai, Gallant, Ishida.

Analysis and interpretation of data. Mukai, Gallant, Ishida, Kittaka, Yoshitaka, Fox, Morita, Nishida, Rottapel, Ueki.

REFERENCES

1. Pettit AR, Ji H, von Steechow D, Muller R, Goldring SR, Choi Y, et al. TRANCE/RANKL knockout mice are protected from bone erosion in a serum transfer model of arthritis. Am J Pathol 2001;159:1689–99.
2. Redlich K, Hayer S, Ricci R, David JP, Tohidast-Akrad M, Kollias G, et al. Osteoclasts are essential for TNF-α-mediated joint destruction. J Clin Invest 2002;110:1419–27.
3. McInnes IB, Schett G. The pathogenesis of rheumatoid arthritis. N Engl J Med 2011;365:2205–19.
4. Redlich K, Smolen JS. Inflammatory bone loss: pathogenesis and therapeutic intervention. Nat Rev Drug Discov 2012;11:234–50.
5. Schett G, Gravallese E. Bone erosion in rheumatoid arthritis: mechanisms, diagnosis and treatment. Nat Rev Rheumatol 2012; 8:656–64.
6. Takayanagi H. New developments in osteoimmunology. Nat Rev Rheumatol 2012;8:684–9.
7. Lam J, Takeshita S, Barker JE, Kanagawa O, Ross FP, Teitelbaum SL. TNF-α induces osteoclastogenesis by direct stimulation of macrophages exposed to permissive levels of RANK ligand. J Clin Invest 2000;106:1481–8.
8. O'Gradaigh D, Ireland D, Bord S, Compston JE. Joint erosion in rheumatoid arthritis: interactions between tumour necrosis factor α, interleukin 1, and receptor activator of nuclear factor κB ligand (RANKL) regulate osteoclasts. Ann Rheum Dis 2004;63:354–9.
9. Fuller K, Murphy C, Kirstein B, Fox SW, Chambers TJ. TNFα potently activates osteoclasts, through a direct action independent of and strongly synergistic with RANKL. Endocrinology 2002;143: 1108–18.
10. Kobayashi K, Takahashi N, Jimi E, Udagawa N, Takami M, Kotake S, et al. Tumor necrosis factor α stimulates osteoclast differentiation by a mechanism independent of the ODF/RANKL-RANK interaction. J Exp Med 2000;191:275–86.
11. Geusens P, Lems WF. Osteoimmunology and osteoporosis. Arthritis Res Ther 2011;13:242.
12. Gough AK, Lilley J, Eyre S, Holder RL, Emery P. Generalised bone loss in patients with early rheumatoid arthritis. Lancet 1994;344:23–7.
13. Vander Cruyssen B, Peene I, Cantaert T, Hoffman IE, De Rycke L, Veys EM, et al. Anti-citrullinated protein/peptide antibodies (ACPA) in rheumatoid arthritis: specificity and relation with rheumatoid factor. Autoimmun Rev 2005;4:468–74.
14. Deckert M, Tartare-Deckert S, Hernandez J, Rottapel R, Altman A. Adaptor function for the Syk kinases-interacting protein 3BP2 in IL-2 gene activation. Immunity 1998;9:595–605.
15. Jevremovic D, Billadeau DD, Schoon RA, Dick CJ, Leibson PJ. Regulation of NK cell-mediated cytotoxicity by the adaptor protein 3BP2. J Immunol 2001;166:7219–28.
16. Levaot N, Simoncic PD, Dimitriou ID, Scotter A, La Rose J, Ng AH, et al. 3BP2-deficient mice are osteoporotic with impaired osteoblast and osteoclast functions. J Clin Invest 2011;121: 3244–57.
17. GuezGuez A, Prod'homme V, Mouska X, Baudot A, Blin-Wakkach C, Rottapel R, et al. 3BP2 adapter protein is required for receptor activator of NFκB ligand (RANKL)-induced osteoclast differentiation of RAW264.7 cells. J Biol Chem 2010;285: 20952–63.
18. Chen G, Dimitriou ID, La Rose J, Ilangumaran S, Yeh WC, Doody G, et al. The 3BP2 adapter protein is required for optimal B-cell activation and thymus-independent type 2 humoral response. Mol Cell Biol 2007;27:3109–22.
19. De la Fuente MA, Kumar L, Lu B, Geha RS. 3BP2 deficiency impairs the response of B cells, but not T cells, to antigen receptor ligation. Mol Cell Biol 2006;26:5214–25.
20. Sada K, Miah SM, Maeno K, Kyo S, Qu X, Yamamura H. Regulation of FcεRI-mediated degranulation by an adaptor protein 3BP2 in rat basophilic leukemia RBL-2H3 cells. Blood 2002;100:2138–44.
21. Ueki Y, Lin CY, Senoo M, Ebihara T, Agata N, Onji M, et al. Increased myeloid cell responses to M-CSF and RANKL cause bone loss and inflammation in SH3BP2 "cherubism" mice. Cell 2007;128:71–83.
22. Tiziani V, Reichenberger E, Buzzo CL, Niazi S, Fukai N, Stiller M, et al. The gene for cherubism maps to chromosome 4p16. Am J Hum Genet 1999;65:158–66.
23. Ueki Y, Tiziani V, Santanna C, Fukai N, Maulik C, Garfinkle J, et al. Mutations in the gene encoding c-Abl-binding protein SH3BP2 cause cherubism. Nat Genet 2001;28:125–6.
24. Papadaki ME, Lietman SA, Levine MA, Olsen BR, Kaban LB, Reichenberger EJ. Cherubism: best clinical practice. Orphanet J Rare Dis 2012;7 Suppl 1:S6.
25. Southgate J, Sarma U, Townend JV, Barron J, Flanagan AM. Study of the cell biology and biochemistry of cherubism. J Clin Pathol 1998;51:831–7.

26. Kawamoto T, Fan C, Gaivin RJ, Levine MA, Lietman SA. Decreased SH3BP2 inhibits osteoclast differentiation and function. J Orthop Res 2011;29:1521–7.
27. Hayward MD, Jones BK, Saparov A, Hain HS, Trillat AC, Bunzel MM, et al. An extensive phenotypic characterization of the hTNFα transgenic mice. BMC Physiol 2007;7:13.
28. Keffer J, Probert L, Cazlaris H, Georgopoulos S, Kaslaris E, Kioussis D, et al. Transgenic mice expressing human tumour necrosis factor: a predictive genetic model of arthritis. EMBO J 1991;10:4025–31.
29. Seki N, Sudo Y, Yoshioka T, Sugihara S, Fujitsu T, Sakuma S, et al. Type II collagen-induced murine arthritis. I. Induction and perpetuation of arthritis require synergy between humoral and cell-mediated immunity. J Immunol 1988;140:1477–84.
30. Cho YG, Cho ML, Min SY, Kim HY. Type II collagen autoimmunity in a mouse model of human rheumatoid arthritis. Autoimmun Rev 2007;7:65–70.
31. Dempster DW, Compston JE, Drezner MK, Glorieux FH, Kanis JA, Malluche H, et al. Standardized nomenclature, symbols, and units for bone histomorphometry: a 2012 update of the report of the ASBMR Histomorphometry Nomenclature Committee. J Bone Miner Res 2013;28:2–17.
32. Proulx ST, Kwok E, You Z, Papuga MO, Beck CA, Shealy DJ, et al. Longitudinal assessment of synovial, lymph node, and bone volumes in inflammatory arthritis in mice by in vivo magnetic resonance imaging and microfocal computed tomography. Arthritis Rheum 2007;56:4024–37.
33. Mukai T, Ishida S, Ishikawa R, Yoshitaka T, Kittaka M, Gallant R, et al. SH3BP2 cherubism mutation potentiates TNF-α-induced osteoclastogenesis via NFATc1 and TNF-α-mediated inflammatory bone loss. J Bone Miner Res 2014;29:618–35.
34. Bouxsein ML, Boyd SK, Christiansen BA, Guldberg RE, Jepsen KJ, Muller R. Guidelines for assessment of bone microstructure in rodents using micro-computed tomography. J Bone Miner Res 2010;25:1468–86.
35. Morita Y, Yang J, Gupta R, Shimizu K, Shelden EA, Endres J, et al. Dendritic cells genetically engineered to express IL-4 inhibit murine collagen-induced arthritis. J Clin Invest 2001;107:1275–84.
36. Brand DD, Latham KA, Rosloniec EF. Collagen-induced arthritis. Nat Protoc 2007;2:1269–75.
37. Inglis JJ, Simelyte E, McCann FE, Criado G, Williams RO. Protocol for the induction of arthritis in C57BL/6 mice. Nat Protoc 2008;3:612–8.
38. Aliprantis AO, Ueki Y, Sulyanto R, Park A, Sigrist KS, Sharma SM, et al. NFATc1 in mice represses osteoprotegerin during osteoclastogenesis and dissociates systemic osteopenia from inflammation in cherubism. J Clin Invest 2008;118:3775–89.
39. Takayanagi H, Kim S, Koga T, Nishina H, Isshiki M, Yoshida H, et al. Induction and activation of the transcription factor NFATc1 (NFAT2) integrate RANKL signaling in terminal differentiation of osteoclasts. Dev Cell 2002;3:889–901.
40. Zhao B, Takami M, Yamada A, Wang X, Koga T, Hu X, et al. Interferon regulatory factor-8 regulates bone metabolism by suppressing osteoclastogenesis. Nat Med 2009;15:1066–71.
41. Yao Z, Xing L, Boyce BF. NF-κB p100 limits TNF-induced bone resorption in mice by a TRAF3-dependent mechanism. J Clin Invest 2009;119:3024–34.
42. Zhao B, Grimes SN, Li S, Hu X, Ivashkiv LB. TNF-induced osteoclastogenesis and inflammatory bone resorption are inhibited by transcription factor RBP-J. J Exp Med 2012;209:319–34.
43. Foucault I, Le Bras S, Charvet C, Moon C, Altman A, Deckert M. The adaptor protein 3BP2 associates with VAV guanine nucleotide exchange factors to regulate NFAT activation by the B-cell antigen receptor. Blood 2005;105:1106–13.
44. Shukla U, Hatani T, Nakashima K, Ogi K, Sada K. Tyrosine phosphorylation of 3BP2 regulates B cell receptor-mediated activation of NFAT. J Biol Chem 2009;284:33719–28.
45. Chen G, Dimitriou I, Milne L, Lang KS, Lang PA, Fine N, et al. The 3BP2 adapter protein is required for chemoattractant-mediated neutrophil activation. J Immunol 2012;189:2138–50.
46. Ainsua-Enrich E, Alvarez-Errico D, Gilfillan AM, Picado C, Sayos J, Rivera J, et al. The adaptor 3BP2 is required for early and late events in FcεRI signaling in human mast cells. J Immunol 2012; 189:2727–34.
47. Hendrich C, Kuipers JG, Kolanus W, Hammer M, Schmidt RE. Activation of CD16+ effector cells by rheumatoid factor complex: role of natural killer cells in rheumatoid arthritis. Arthritis Rheum 1991;34:423–31.
48. Cross A, Bucknall RC, Cassatella MA, Edwards SW, Moots RJ. Synovial fluid neutrophils transcribe and express class II major histocompatibility complex molecules in rheumatoid arthritis. Arthritis Rheum 2003;48:2796–806.
49. Malone DG, Wilder RL, Saavedra-Delgado AM, Metcalfe DD. Mast cell numbers in rheumatoid synovial tissues: correlations with quantitative measures of lymphocytic infiltration and modulation by antiinflammatory therapy. Arthritis Rheum 1987;30: 130–7.
50. Wang CJ, Chen IP, Koczon-Jaremko B, Boskey AL, Ueki Y, Kuhn L, et al. Pro416Arg cherubism mutation in Sh3bp2 knock-in mice affects osteoblasts and alters bone mineral and matrix properties. Bone 2010;46:1306–15.